

Search for lepton flavor violation process $e^+e^- \rightarrow e\mu$ in the energy region $\sqrt{s} = 984\text{--}1060$ MeV and $\phi \rightarrow e\mu$ decay

M. N. Achasov,* K. I. Beloborodov, A. V. Bergyugin, A. G. Bogdanchikov, A. D. Bukin, D. A. Bukin, T. V. Dimova, V. P. Druzhinin, V. B. Golubev, I. A. Koop, A. A. Korol, S. V. Koshuba, A. P. Lysenko, E. V. Pakhtusova, S. I. Serednyakov, Yu. M. Shatunov, Z. K. Silagadze, A. N. Skrinsky, and A. V. Vasiljev

Budker Institute of Nuclear Physics, Siberian Branch of the Russian Academy of Sciences, 11 Lavrentyev, Novosibirsk, 630090, Russia, and Novosibirsk State University, 630090, Novosibirsk, Russia

(Received 8 November 2009; revised manuscript received 26 February 2010; published 29 March 2010)

A search for lepton-flavor-violating process $e^+e^- \rightarrow e\mu$ in the energy region $\sqrt{s} = 984\text{--}1060$ MeV with the SND detector at the VEPP-2M e^+e^- collider is reported. The model independent 90% C.L. upper limits on the $e^+e^- \rightarrow e\mu$ cross section, $\sigma_{e\mu} < 8$ pb, as well as on the corresponding $\phi \rightarrow e\mu$ branching fraction, $B(\phi \rightarrow e\mu) < 2 \times 10^{-6}$ have been obtained, for the polar angles $55^\circ < \theta < 125^\circ$ of the final particles.

DOI: 10.1103/PhysRevD.81.057102

PACS numbers: 13.20.Jf, 13.66.De

For most of the fundamental fermions (quarks and neutrinos), the processes with flavor violation, quark decays, and neutrino oscillations are known. At the same time, the lepton-flavor-violating (LFV) processes involving charged leptons have never been observed. Theoretically, the processes of this kind are not strictly forbidden and can occur in many extensions of the standard model.

For a LFV hunting, decays of μ and τ leptons, as well as of the Z boson and various quark-antiquark mesons (K , B , D , η , J/ψ , Y), along with a conversion process $\mu N \rightarrow eN$ have already been used [1,2]. The annihilation processes $e^+e^- \rightarrow e\mu$, $e\tau$, $\mu\tau$ are also suitable for this purpose. Theoretically, these processes and related gauge boson and vector meson decays were studied, for example, in [3]. On the experimental side, the searches for the decays $J/\psi \rightarrow e\mu$, $e\tau$, $\mu\tau$ [4], $Y \rightarrow \mu\tau$ [5], $Z \rightarrow e\mu$, $e\tau$, $\mu\tau$ [6], as well as for the annihilation processes $e^+e^- \rightarrow e\tau$, $\mu\tau$ in the $Y(4S)$ energy range [7], and for the processes $e^+e^- \rightarrow e\mu$, $e\tau$, $\mu\tau$ in the energy range $\sqrt{s} = 189\text{--}209$ GeV [8] were performed. However, in the energy region below the J/ψ production threshold such studies have not yet been done. In the $\phi(1020)$ -meson energy range, it is possible to search for the LFV process $e^+e^- \rightarrow e\mu$ and the corresponding decay $\phi \rightarrow e\mu$ (Fig. 1).

Existing stringent bounds on LFV $\mu \rightarrow 3e$ decay can be transformed into a strict constraint on the two-body $\phi \rightarrow e\mu$ branching fraction: $B(\phi \rightarrow e\mu) \leq 4 \times 10^{-17}$ unless some magic cancellations take place in the $\mu \rightarrow 3e$ decay amplitude [9]. At first sight, such a strong constraint makes doubtful any experimental effort to search for this decay. However, a possibility of cancellations mentioned above, although rather unlikely, cannot be absolutely excluded.

This work reports the results of a study of the process $e^+e^- \rightarrow e\mu$ in the energy region $\sqrt{s} \sim 1$ GeV with the SND detector at the VEPP-2M collider e^+e^- .

The SND detector [10] operated from 1995 to 2000 at the VEPP-2M [11] collider in the energy range \sqrt{s} from 360 to 1400 MeV. The detector contains several subsystems. The tracking system includes two cylindrical drift chambers. The three-layer spherical electromagnetic calorimeter is based on NaI(Tl) crystals. The muon system consists of plastic scintillation counters and two layers of streamer tubes. The calorimeter energy resolution for 500 MeV electrons is about 5%. The azimuthal and polar angles of charged particles are measured by the tracking system with a resolution of about 0.5° and 2° . SND is not operating in a magnetic field, thus the tracking system is only used to measure the impact parameters and angles of tracks.

This work is based on the data collected in the scans of the ϕ -meson energy region. The total integrated luminosity used is $IL = 8.5 \text{ pb}^{-1}$. The luminosity was measured using the process $e^+e^- \rightarrow e^+e^-$ with the accuracy of about 2% [12].

In the reaction $e^+e^- \rightarrow e\mu$, the final particles are detected by the tracking system and have substantively different energy depositions in the calorimeter. The muon system detects muons with a probability greater than 90%, while electrons are detected by this system with the probability less than 0.2%. To search for the $e^+e^- \rightarrow e\mu$ process, so-called collinear events containing two charged particles were used. We assume that the charged particle

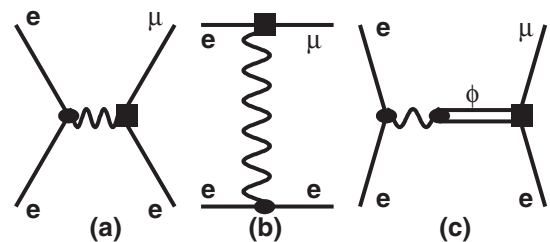


FIG. 1. The diagrams of the $e^+e^- \rightarrow e\mu$ process.

*achasov@inp.nsk.su

with higher energy deposition in the calorimeter (particle number one) is an electron, while that with lower energy deposition (particle number two) is a muon. Events were selected using the following criteria (subscripts 1 and 2 denote the particle number):

- (1) $N_{\text{cha}} = 2$, where N_{cha} is the number of charged particles originated from the interaction point: $|z_{1,2}| < 10$ cm and $r_{1,2} < 1$ cm. Here z is the coordinate of the charged particle production point along the beam axis (the longitudinal size of the interaction region σ_z is about 2.5 cm), r is the distance between the charged particle track and the beam axis in the $r - \phi$ plane;
- (2) $|\Delta\theta| = |180^\circ - (\theta_1 + \theta_2)| < 10^\circ$, where θ is the particle polar angle;
- (3) $|\Delta\phi| = |180^\circ - |\phi_1 - \phi_2|| < 10^\circ$, where ϕ is the particle azimuthal angle;
- (4) $55^\circ < \theta_{1,2} < 125^\circ$ (this angular region is covered with the muon system);
- (5) the angular region $240^\circ < \phi_{1,2} < 300^\circ$ not covered with the muon system was excluded;
- (6) there is a hit in the muon system from the second particle while there is no hit from the first one;
- (7) $20 < E_2^I < 50$ MeV, $40 < E_2^{II} < 80$ MeV, and $50 < E_2^{III} < 90$ MeV, where E_i^j are the energy depositions in the calorimeter layers, i denotes the particle number and $j = I, II, III$ is the layer number;
- (8) $E_1^I > 70$ MeV, $E_1^{II} > 130$ MeV, and $20 < E_1^{III} < 100$ MeV.

As a result, 146 events were selected. The visible cross section (the event number divided by the integrated luminosity) varies weakly with beam energy. No contribution from the ϕ -meson decays $\phi \rightarrow K^+ K^-$, $K_S K_L$, $\pi^+ \pi^- \pi^0$ is seen. This agrees with the expectations from the Monte-Carlo (MC) simulation. The background from the $e^+ e^- \rightarrow e^+ e^-$ process is negligible, only two events are expected. Events from the background process $e^+ e^- \rightarrow \pi^+ \pi^-$ can pass the selection if one of the pions loses its energy due to ionization, while the other pion—due to nuclear interactions.

In order to obtain the cross section of the process $e^+ e^- \rightarrow e\mu$ in the whole energy region $\sqrt{s} = 984\text{--}1060$ MeV, the E_e^*/E_e distribution (Fig. 2) was analyzed. Here E_e^* and E_e are the electron energies measured by the calorimeter and expected from the process kinematics, respectively. To obtain the number of $e^+ e^- \rightarrow e\mu$ events ($N_{e\mu}$), the E_e^*/E_e spectrum was fit by a sum of distributions for electrons and background. The distribution for electrons was obtained using experimental $e^+ e^- \rightarrow e^+ e^-$ events in the following way. The $e^+ e^- \rightarrow e^+ e^-$ events were selected using criteria 1–5 and requiring that the muon system was not fired by any particle and that the energy deposition of a randomly chosen particle was greater than $0.85 \times E_0$ (E_0 is the beam energy). The sec-

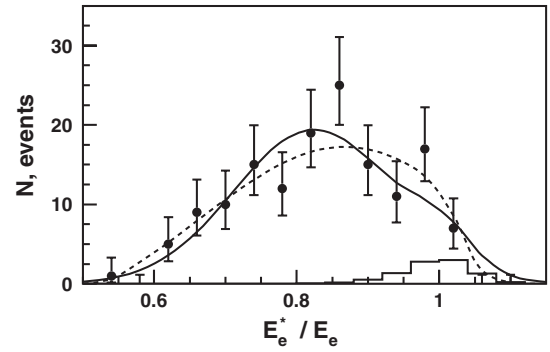


FIG. 2. Ratio E_e^*/E_e between the measured energy E_e^* of the electron candidate and the energy E_e expected from kinematics in case of an $e\mu$ event. Dots represent experimental data. The solid curve is the result of a fit with the sum of the distribution for electrons (histogram) and a Gaussian. The dashed curve is the result of a fit with the sum of the distribution for electrons (histogram) and a third-order polynomial.

ond particle in the event was used to obtain the distribution. The background was approximated either by a Gaussian function or by a third-order polynomial. The coefficients of the background function and $N_{e\mu}$ were free parameters of the fit. When the background was approximated with a Gaussian, it was found that

$$N_{e\mu} = 12 \pm_{16}^{14}.$$

This corresponds to the upper limit

$$N_{e\mu} < 21 \quad \text{C.L.} = 90\%.$$

In the case of a third-order polynomial it was obtained that

$$N_{e\mu} = 7 \pm_{9}^{11}.$$

The corresponding upper limit is

$$N_{e\mu} < 14 \quad \text{C.L.} = 90\%.$$

The upper limits were obtained using a toy Monte Carlo study [13]. The higher limit $N_{e\mu} < 21$ was used for the further considerations.

The detection efficiency of the tracking system for $e^+ e^- \rightarrow e\mu$ events, $\varepsilon_{\text{track}}$ (cuts 1–5), was obtained from MC simulation [10,14]. MC events were generated with a $1 + \cos^2\theta$ distribution. The detection efficiency obtained for the angular region $55^\circ < \theta < 125^\circ$ actually does not depend on the model of the θ distribution and is equal to $\varepsilon_{\text{track}} = 0.59$. The experimental and simulated θ , $\Delta\theta$, and $\Delta\phi$ distributions for the processes $e^+ e^- \rightarrow e^+ e^-$, $e^+ e^- \rightarrow \pi^+ \pi^-$, $e^+ e^- \rightarrow \mu^+ \mu^-$ are in good agreement [12,14]. The systematic uncertainty associated with the $\varepsilon_{\text{track}}$ determination is estimated to be less than 3%.

The efficiencies of muon and electron detection by the muon system were obtained using $e^+ e^- \rightarrow \mu^+ \mu^-$ and $e^+ e^- \rightarrow e^+ e^-$ data events. The $e^+ e^- \rightarrow \mu^+ \mu^-$ events were selected according to the criteria 1–5 described

above. The additional cut $r_{1,2} < 0.1$ cm was used for suppression of the cosmic ray background. The cut 7 was imposed on both particles. One particle was required to hit the muon system, while the other particle was used to determine the detection efficiency. The residual cosmic background was subtracted using the distribution of the z coordinate of the particles production point [12]. The detection efficiency $\varepsilon_{\text{muon}}^{\mu}$ depends on the muon energy. Its value varies from 0.90 to 0.95 with the average value of $\varepsilon_{\text{muon}}^{\mu}$ equal to 0.94. $e^+e^- \rightarrow e^+e^-$ events were selected by the cuts 1–5 and the condition $E_{1,2}/E_0 > 0.7$. It was found that $1 - \varepsilon_{\text{muon}}^e = 0.998$.

Probabilities for muons and electrons to pass a condition on the energy deposition in the calorimeter were obtained in a similar way. $e^+e^- \rightarrow \mu^+\mu^-$ events were selected using cuts 1–5 and additional requirements $r_{1,2} < 0.2$ cm, $E_{1,2}/E_0 < 0.6$. It was required that the muon system was hit by both particles. The cosmic background was suppressed by the restriction $|\tau_1 - \tau_2| < 5$ ns, where $\tau_{1,2}$ are time intervals between the signals from the scintillation counters and the beam collision moment. The probability for muons to pass cut 7 was found to be $\varepsilon_{\text{cal}}^{\mu} = 0.86$. The $e^+e^- \rightarrow e^+e^-$ events were selected using criteria 1–5 and requiring that the muon system was not fired by any particle and that the energy deposition of a randomly chosen particle was greater than $0.85 \times E_0$. Another particle was used to obtain a probability to satisfy the criterion 8, $\varepsilon_{\text{cal}}^e = 0.70$. The values of $\varepsilon_{\text{cal}}^{\mu}$ and $\varepsilon_{\text{cal}}^e$ do not depend on the beam energy.

The detection efficiency of the $e^+e^- \rightarrow e\mu$ process was calculated as follows:

$$\varepsilon_{e\mu} = \varepsilon_{\text{track}} \varepsilon_{\text{muon}}^{\mu} (1 - \varepsilon_{\text{muon}}^e) \varepsilon_{\text{cal}}^{\mu} \varepsilon_{\text{cal}}^e$$

and the $e^+e^- \rightarrow e\mu$ cross section as

$$\sigma_{e\mu} = \frac{N_{e\mu}}{IL\varepsilon_{e\mu}},$$

where $N_{e\mu} < 21$, $\varepsilon_{e\mu} = 0.31$ (the average value $\varepsilon_{\text{muon}}^{\mu} = 0.94$ was used), $IL = 8.5 \text{ pb}^{-1}$. The following upper limit for the angular region $55^\circ < \theta < 125^\circ$ was obtained:

$$\sigma_{e\mu} < 8 \text{ pb} \quad \text{C.L.} = 90\%.$$

The upper limit on the $\phi \rightarrow e\mu$ decay was obtained assuming absence of any nonresonance contribution and by using the additional cut $0.9 < E_e^*/E_0 < 1.1$ (then $\varepsilon_{\text{cal}}^e = 0.64$). The energy dependence of the visible cross section is

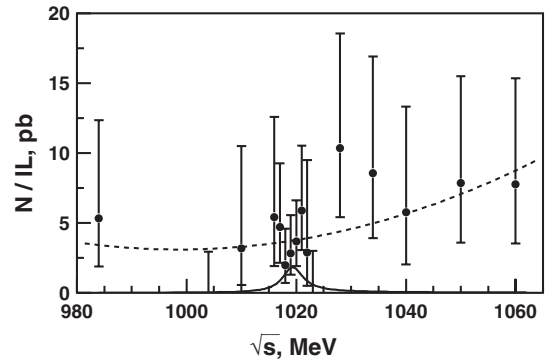


FIG. 3. The visible cross section obtained after the additional cut $0.9 < E_e^*/E_0 < 1.1$. The solid curve is the expected resonance line shape corresponding to the upper limit on $B(\phi \rightarrow e\mu)$, the dashed curve is a background approximation.

shown in Fig. 3. It was fit by the function

$$\sigma = \varepsilon_{e\mu} (1 + \delta_{\text{rad}}) \frac{4\pi\alpha^2}{3s} \left| \frac{3}{\alpha} \sqrt{B(\phi \rightarrow e^+e^-)B(\phi \rightarrow e\mu)} \times \frac{m_\phi \Gamma_\phi}{m_\phi^2 - s - i\sqrt{s}\Gamma_\phi(s)} \right|^2 + P_2(s), \quad (1)$$

where $(1 + \delta_{\text{rad}})$ is the radiative correction factor [15], $P_2(s)$ is a second-order polynomial describing the background, m_ϕ , $\Gamma_\phi(s)$ are the ϕ -meson mass and energy dependent total width [16], respectively, and $\Gamma_\phi = \Gamma_\phi(m_\phi^2)$. The beam energy spread (0.37 MeV) and the error in the beam energy determination (0.04 MeV) were taken into account in the fit [17]. The branching ratio and the coefficients of the $P_2(s)$ were free fit parameters. For the angular region $55^\circ < \theta < 125^\circ$, it was obtained that

$$B(\phi \rightarrow e\mu) = (0.0 \pm 1.5) \times 10^{-6},$$

which corresponds to the upper limit

$$B(\phi \rightarrow e\mu) < 2 \times 10^{-6} \quad \text{C.L.} = 90\%.$$

The presented upper limits do not depend on the angular distribution of the process $e^+e^- \rightarrow e\mu$.

The authors are grateful to S.I. Eidelman for useful discussions. The work is supported in part by RF Presidential Grant for Scientific School NSH-5655.2008.2, and by RFBR Grants No. 08-02-00328-a, No. 08-02-00634-a, and No. 08-02-00660-a.

- [1] W.J. Marciano, T. Mori, and J.M. Roney, *Annu. Rev. Nucl. Part. Sci.* **58**, 315 (2008).
 [2] L.G. Landsberg, *Yad. Fiz.* **68**, 1240 (2005) [*Phys. At. Nucl.* **68**, 1190 (2005)]; P. Depommier and C. Leroy, *Rep.*

- Prog. Phys.* **58**, 61 (1995); J.L. Feng, arXiv:hep-ph/0101122; T. Mori, arXiv:hep-ex/0605116.
 [3] Z.K. Silagadze, *Phys. Scr.* **64**, 128 (2001); P.M. Ferreira, R.B. Guedes, and R. Santos, *Phys. Rev. D* **75**, 055015

- (2007); Z. T. Wei, Y. Xu, and X. Q. Li, *Eur. Phys. J. C* **62**, 593 (2009); M. Cannoni, S. Kolb, and O. Panella, *Phys. Rev. D* **68**, 096002 (2003); C. D. Lu, W. Wang, and Y. M. Wang, *Phys. Rev. D* **76**, 077701 (2007); Y. B. Sun, L. Han, W. G. Ma, F. Tabbakh, R. Y. Zhang, and Y. J. Zhou, *J. High Energy Phys.* 09 (2004) 043; C. X. Yue, Y. M. Zhang, and H. Li, *J. Phys. G* **29**, 737 (2003); E. O. Iltan and I. Turan, *Phys. Rev. D* **65**, 013001 (2001).
- [4] J. Z. Bai *et al.* (BES Collaboration), *Phys. Lett. B* **561**, 49 (2003); M. Ablikim *et al.* (BES Collaboration), *Phys. Lett. B* **598**, 172 (2004).
- [5] W. Love *et al.* (CLEO Collaboration), *Phys. Rev. Lett.* **101**, 201601 (2008).
- [6] M. Z. Akrawy *et al.* (OPAL Collaboration), *Phys. Lett. B* **254**, 293 (1991); D. Decamp *et al.* (ALEPH Collaboration), *Phys. Rep.* **216**, 253 (1992); P. Abreu *et al.* (DELPHI Collaboration), *Phys. Lett. B* **298**, 247 (1993); O. Adriani *et al.* (L3 Collaboration), *Phys. Lett. B* **316**, 427 (1993).
- [7] B. Aubert *et al.* (BABAR Collaboration), *Phys. Rev. D* **75**, 031103 (2007).
- [8] G. Abbiendi *et al.* (OPAL Collaboration), *Phys. Lett. B* **519**, 23 (2001).
- [9] S. Nussinov, R. D. Peccei, and X. M. Zhang, *Phys. Rev. D* **63**, 016003 (2000).
- [10] M. N. Achasov *et al.*, *Nucl. Instrum. Methods Phys. Res., Sect. A* **449**, 125 (2000).
- [11] A. N. Skrinsky, in *Proceedings of the Workshop on Physics and Detectors for DAΦNE*, Frascati Physics Series Vol. 4 (INFN Laboratori Nazionali di Frascati, Frascati, Italy, 1995), p. 3.
- [12] M. N. Achasov *et al.*, *Phys. Rev. D* **79**, 112012 (2009).
- [13] R. Barlow, in *Proceedings of the PHYSTAT2003: Statistical Problems in Particle Physics, Astrophysics, and Cosmology* (Stanford, Menlo Park, California, 2003), pp. MOAT002; *Comput. Phys. Commun.* **149**, 97 (2002).
- [14] M. N. Achasov *et al.*, *Zh. Eksp. Teor. Fiz.* **128**, 1201 (2005) [*J. Exp. Theor. Phys.* **101**, 1053 (2005)].
- [15] E. A. Kuraev and V. S. Fadin, *Yad. Fiz.* **41**, 733 (1985) [*Sov. J. Nucl. Phys.* **41**, 466 (1985)].
- [16] M. N. Achasov *et al.*, *Phys. Rev. D* **63**, 072002 (2001).
- [17] A. V. Bozhenok *et al.*, Report No. Budker INP 99-103, 1999.